APPLIED PHYSICS LETTERS **92**, 241109 (2008)

Green light emitting diodes on *a*-plane GaN bulk substrates

Theeradetch Detchprohm,[1,a] Mingwei Zhu,[1] Yufeng Li,[1] Yong Xia,[1] Christian Wetzel,[1] Edward A. Preble,[2] Lianghong Liu,[2] Tanya Paskova,[2] and Drew Hanser[2]
[1]*Future Chips Constellation, and Department of Physics, Applied Physics and Astronomy, Rensselaer Polytechnic Institute, Troy, New York 12180, USA*
[2]*Kyma Technologies, Inc., 8829 Midway West Road, Raleigh, North Carolina 27617, USA*

(Received 6 May 2008; accepted 27 May 2008; published online 17 June 2008)

We report the development of 520–540 nm green light emitting diodes (LEDs) grown along the nonpolar *a* axis of GaN. GaInN/GaN-based quantum well structures were grown in homoepitaxy on both, *a*-plane bulk GaN and *a*-plane GaN on *r*-plane sapphire. LEDs on GaN show higher, virtually dislocation-free crystalline quality and three times higher light output power when compared to those on *r*-plane sapphire. Both structures show a much smaller wavelength blue shift for increasing current density (<10 nm for 0.1 to 12.7 A/cm^2) than conventional LEDs grown along the polar *c* axis. © *2008 American Institute of Physics*. [DOI: 10.1063/1.2945664]

The uniaxial crystallographic structure of wurtzite group-III nitrides induces a piezoelectric dipole across the *c*-axis oriented GaInN/GaN quantum well (QW), which is typically used in the active region of light emitting diodes (LEDs) and laser diodes. The associated electric field leads to a longer emission wavelength and a spatial separation of electron and hole wave functions.[1,2] This separation reduces the interband transition matrix element [the so-called quantum confined Stark effect (QCSE)] and may be responsible for a reduced efficiency in longer wavelength LEDs. For example, 450 nm blue LEDs can achieve an external quantum efficiency (EQE: ratio of photons emitted to electrons injected) of 30%–40%, while records for 525 nm green LEDs merely reach 20%.[3] This should be due to the higher InN fraction and larger polarization dipole. In order to enhance device efficiency, Takeuchi *et al.* proposed to avoid piezoelectric polarization by employing epitaxial growth of the QWs along crystallographic directions with lower polarization such as $[11\bar{2}4]$, or without polarization such as $[10\bar{1}0]$ *m* axis and $[11\bar{2}0]$ *a* axis.[4]

In their work,[4,5] they used the inclined $\{10\bar{1}1\}$ planes of anisotropically overgrown but not fully coalesced *c*-plane stripes, leaving small nonpolar side surfaces. Nonpolar *a*-plane $(11\bar{2}0)$ GaN can be obtained in large areas by heteroepitaxy on *r*-plane $(1\bar{1}02)$ sapphire.[6] However, threading and misfit dislocation densities in these structures are as high as in *c*-axis heteroepitaxial ones and therefore require elaboration of techniques to stop their penetration of the active region.[7,8] LED structures, grown by these approaches, have been reported covering emission from the UV to the green (525 nm).[9–11] So far, however, their light output performance is far below what has been achieved in *c*-axis material. Likely reasons are the high density of threading dislocations (TDs) and poorly optimized device structures.[10,11]

Meanwhile, low-dislocation-density, freestanding *c*-axis GaN substrate has become commercially available at sizes up to 2 in. diameter. Grown at high growth rate in hydride vapor phase epitaxy (HVPE), TD densities in the mid 10^6 cm^{-2} are repeatedly achieved.[12] Nonpolar bulk GaN substrates in reasonable size can then be obtained by slicing a centimeter-thick HVPE-GaN boule along *a* and *m* planes. This approach provides a low-dislocation-density template for epitaxial growth along these nonpolar axes. For *m*-plane substrates, benefits have been shown for UV and blue LEDs (Refs. 13 and 14) and laser diodes.[15–17] For *a*-plane substrates, blue LEDs have been reported.[18,19]

Here we report the development of nonpolar green LEDs grown on low-dislocation-density *a*-plane bulk GaN. The characteristics and performance of these devices are discussed and compared to those grown on *r*-plane sapphire (nonpolar LED) and *c*-plane sapphire (polar LED).

GaN bulk templates with an *a*-plane surface, 450 μm in thickness and 5×10 mm^2 in size were sliced from thick GaN boules grown along (0001) by HVPE. A chemomechanical polishing process was applied to achieve an atomically flat *a*-plane surface [surface roughness $\leqslant 0.5$ nm root mean square (rms)], with a well-controlled crystal orientation (misorientation is within $\pm 2°$ of the *a* axis). The device structures grown along the *a* axis include a 1 μm thick Si doped *n*-GaN layer and five periods of 3 nm thick undoped $Ga_{1-x}In_xN$ QW layer and 19 nm thick undoped GaN barrier as the multiple QW (MQW) active region. The InN fractions (x) were gradually increased in order to achieve a light emission wavelength of 520 nm and beyond. By a proper optimization of the metal organic vapor phase epitaxy (MOVPE) growth conditions, *V*-defect formation in the active region was avoided. Further details on the growth process have been given in Ref. 20. A sequence of an 18 nm thick Mg doped *p*-$Al_{0.14}Ga_{0.86}N$ electron blocking layer and a 190 nm thick Mg doped *p*-GaN layer formed the *p* layers on top (type A). For comparison, the same structure was grown on a 6 μm thick *a*-plane GaN layer on *r*-plane sapphire (type B).

The surface morphology of the active region was analyzed by atomic force microscopy (AFM) and secondary electron microscopy (SEM) techniques in areas of 5×5 μm^2. In AFM, type-A samples reveal uniform atomic growth steps aligned parallel to the *c* plane. On the larger scale of SEM, triangular shaped surface pits 3–5 μm in diameter appear at a density of 7.3×10^4 cm^{-2}. Their size and density suggest that they originate in the *n*-GaN layer

[a]Author to whom correspondence should be addressed. Electronic mail: detcht@rpi.edu.

 © 2008 American Institute of Physics
Downloaded 03 Sep 2009 to 128.113.121.60. Redistribution subject to AIP license or copyright; see http://apl.aip.org/apl/copyright.jsp

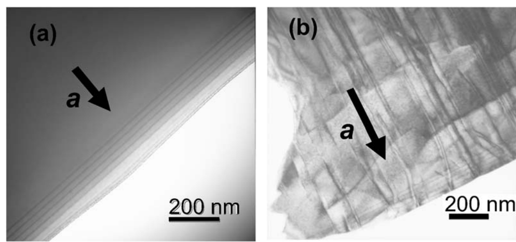

FIG. 1. Transmission electron microscope images of type-A (a) and type-B (b) LED samples. The zone axes are $[10\bar{1}0]$ and [0001], respectively. The TD density is $\leq 10^7$ cm^{-2} in type-A LED structure grown on bulk GaN and as high as 2×10^{10} cm^{-2} in type-B LED structure grown on *r* sapphire. Vector **a** indicates the *a*–axis growth direction.

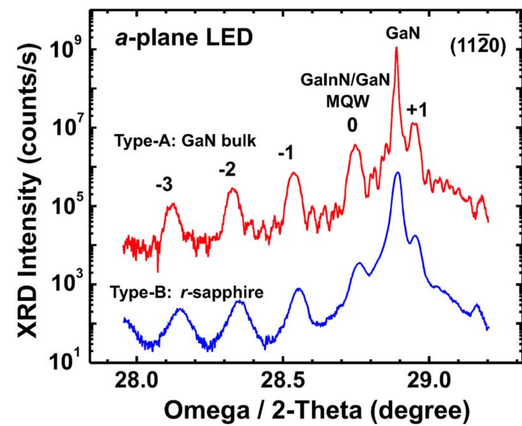

FIG. 2. (Color online) $\Omega/2\theta$ XRD scan around the GaN $11\bar{2}0$ diffraction in nonpolar LED structures of type-A grown on bulk GaN (a) and type-B grown on *r* sapphire (b) substrates.

prior to the MQW growth, possibly initiated by defects in the GaN bulk substrate. In separate samples of full LED structures, the *p*-layer surface shows a high pit density of $(1-3)\times10^8$ cm^{-2} with diameters of 100–200 nm, each. In type-A samples, the surface roughness of both, the MQW samples and LED samples in AFM was found to be in the range of 1.2–3.0 nm (rms) with *z*-range values of 12–22 nm. These values are close to those in our typical green LEDs grown along the *c* axis. On the surface of type-B MQW samples, however, there is a high density of pinhole defects $(9.2\times10^8$ $cm^{-2})$ at a diameter of 20–50 nm, each. Consequently, there is a large surface roughness of 7 nm (rms) with *z*-range values of 50–60 nm. The *p* layer of the corresponding full LED structure samples shows pits of 100–200 nm diameter and density of 8.8×10^8 cm^{-2} and a large surface roughness of 13 nm (rms).

Cross-sectional transmission electron micrographs (TEM) of type-A and type-B samples are shown in Fig. 1 (acceleration voltage 120 kV). It can be seen that type-A LEDs [Fig. 1(a)] inherit the high crystalline quality of the GaN bulk substrate without generation of any additional TDs during the process of homoepitaxy. Under high-resolution TEM analysis, the average thickness of the GaInN QW is estimated to be 2.75 ± 0.25 nm. On the other hand, in type-B samples [Fig. 1(b)], a large density $(2\times10^{10}$ $cm^{-2})$ of TDs can be seen to propagate throughout the device structure from the underlying *a*-plane GaN template. Despite the high defect density, there are no additional epitaxial defects, such as *V* defects, induced in the subsequent epitaxial layers.

In x-ray diffraction (XRD) using the Cu $K\alpha1$ line in a $\omega/2\theta$ scan around the $(11\bar{2}0)$ diffraction of GaN provides fine details (Fig. 2). In type-A samples, satellite peaks appear with well-resolved intermediate fringes. These result from the interference of the individual QWs with the *p*-side layers. Their appearance indicates abrupt interfaces in all layers and uniform composition. In contrast, the absence of such fringes in type-B LED structures suggests poor interface quality and/or composition inhomogeneity. These XRD results are in good agreement with the results from the surface morphology and TEM analysis.

In order to determine the InN fraction of the QWs, we adopt the model of Tsuda *et al.* for determination of the AlN fraction in AlGaN grown on *a*-plane GaN.[21] Within the ternary layer, an anisotropic in-plane strain is assumed and shear forces are neglected. Therefore, the growth *a* axis remains stress-free. Under these assumptions, the alloy composition can be determined. Applying the model to the coherently grown GaInN/GaN MQW, we distinguish lattice periods parallel and perpendicular to the in-plane *c* axis. They can be expressed in terms of the constants c_{GaN} (along *c* axis) and a_{GaN} (along *a* axis) of the underlying GaN layer as c_{GaN} and $\sqrt{3}a_{GaN}/2$, respectively. The lattice constant of the $(11\bar{2}0)$ plane separation $d_{(11\bar{2}0)\mathrm{GaInN}}$ in the QW can then be expressed as 2 $d_{(11\bar{2}0)\mathrm{GaInN}}$. Its value can be determined from the zeroth-order superlattice peak of the MQW structure. In this model, the elastic stiffness constants of the $Ga_{1-x}In_xN$ alloys are linearly interpolated from those of GaN and InN.[21,22] Using an average QW thickness as obtained from the high-resolution TEM analysis, the InN fraction was determined to be 14% in the 3.7 nm thick QWs of type-A and type-B MQW samples that achieve light emission near 500 nm (Table I). In comparison, our 3.0 nm compressively strained QWs grown along the *c* axis of GaN require an InN fraction of merely 7.7% to reach the same wavelength range. Apparently, the InN fraction needed for a green LED in nonpolar growth geometry is roughly twice as high. This can, in part, be explained by the disappearance of the QCSE. According to our previous findings,[2] the disappearing dipole across the QW should alleviate the large Stokes-like redshift in the emission spectrum.

TABLE I. InN fractions of the $Ga_{1-x}In_xN$ QW layers for type-A and type-B samples and their reference samples grown along the *c* axis of GaN. *Zw* is the QW thickness.

Sample	Wavelength (nm), peak type	*Zw* (nm)	InN-fractions(%) Fully strained	Relaxed
Type-A MQW (PL)	503, peak	3.7	13.5	20.2
Type-B MQW (PL)	517, peak	3.7	14.3	23.6
c-axis MQW (PL)	501, peak	3.0	7.7	21.7
Type-A LED (EL)	527, dominant	2.8	18.8	31.1
Type-B LED (EL)	539, dominant	3.7	18.1	30.7
c-axis LED (EL)	524, dominant	3.0	9.0	23.9

Downloaded 03 Sep 2009 to 128.113.121.60. Redistribution subject to AIP license or copyright; see http://apl.aip.org/apl/copyright.jsp

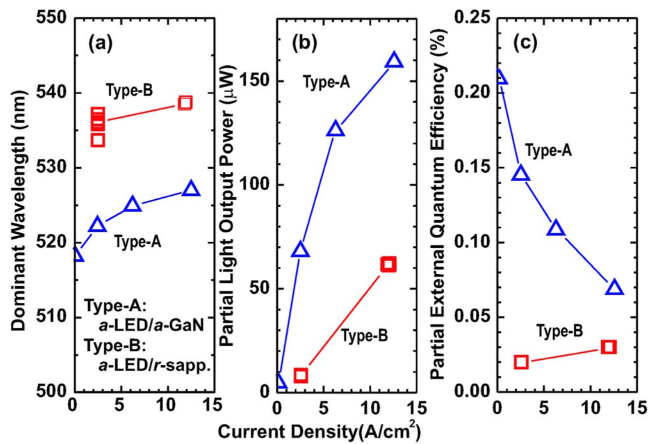

FIG. 3. (Color online) EL characteristics of type-A LED structure grown on bulk GaN and of type-B LED structure grown on *r*-sapphire LEDs as a function of dc current density: (a) dominant wavelength, (b) partial light output power (EQE), and (c) partial external quantum efficiency. Partial refers to the fraction that can be measured through the substrate of the epi wafers. Solid lines are guides to the eye.

Similar results were obtained in electroluminescence (EL) spectra. Dominant emission wavelengths of 525 nm or larger are achieved in polar LED structures grown along the *c* axis for InN-fractions of ~9%. In nonpolar type-A and type-B LED structures, the same wavelengths can be achieved for $x=18.8\%$ and 18.0%, respectively. The correlation of alloy fractions as derived from the XRD analysis and the emission wavelength in PL and EL is summarized in Table I.

Both type-A and type-B LEDs show a single narrow EL emission line in the green range: dominant wavelength of 520–540 nm [Fig. 3(a)] and linewidth of 38–48 nm. The partial optical output power measured through the substrate of the epi wafers reaches 60 μW at a current density of 12.7 A/cm^2 in the type-B LED structures on *r* sapphire, while a threefold higher value of 160 μW is reached in the type-A structures on bulk GaN [Fig. 3(b)]. The (partial) EQE of type-A LEDs shows a monotonic decrease as a function of dc current density [Fig. 3(c)]. Within this current range, the values are consistently several times higher than those obtained in type-B LEDs. As the drive current increases, there is a red shift ($\leq$10 nm) in the dominant wavelength for both, type-A and type-B LEDs, as seen in Fig. 3(c). We attribute the better device performance of type-A LEDs to the higher crystalline quality when compared to type-B LEDs. However, the (partial) EQE of these nonpolar devices is still an order of magnitude lower than that obtained from polar (0001) green GaInN/GaN LEDs. Most likely, this is due to the early development stage of these devices and could possibly be improved with better junction placement. At the current low efficiency level, we cannot precisely distinguish possible thermal effects from the system-inherent effects in the drop of EQE with increasing current density. The observed redshift of the emission wavelength suggests a dominance of the thermal effects.

In conclusion, the crystalline quality and the electro-optical performance of green LEDs grown along the nonpolar *a* axis of GaN has been significantly improved by employing low-dislocation-density *a*-plane $(11\bar{2}0)$ GaN bulk substrates. We observed a threefold increase in light output power when compared to those on high-dislocation-density *a*-plane GaN grown on *r*-plane sapphire, although the overall power still is lower than that obtained in conventional *c*-plane device structures. We found that the InN fractions in the nonpolar QW have to be twice as high as in polar (0001) *c*-axis growth to reach the 500–540 nm green emission region. We attribute this to the elimination of the piezoelectric dipole across the QWs.

This work was supported by a DOE/NETL Solid-State Lighting Contract of Directed Research under Grant No. DE-FC26-06NT42860 and the DARPA VIGIL program through the United States Air Force AFRL/SNH under Grant No. FA8718-08-C-0004.

[1]T. Takeuchi, S. Sota, M. Katsuragawa, M. Komori, H. Takeuchi, H. Amano, and I. Akasaki, Jpn. J. Appl. Phys., Part 2 **36**, L382 (1997).
[2]C. Wetzel, T. Takeuchi, H. Amano, and I. Akasaki, Phys. Rev. B **62**, R13302 (2000).
[3]Report of the Basic Energy Sciences Workshop on Solid-State Lighting, 22–24 May 2006 (unpublished).
[4]T. Takeuchi, H. Amano, and I. Akasaki, Jpn. J. Appl. Phys., Part 1 **39**, 413 (2000).
[5]T. Takeuchi, S. Lester, D. Basile G. Girolami, R. Twist, F. Mertz, M. Wong, R. Schneider, H. Amano, and I. Akasaki, Procceeding of the International Workshop on Nitride Semiconductors, IPAP Conference Series 1, Nagoya, 2000 (unpublished), pp. 137–140.
[6]M. D. Craven, S. H. Lim, F. Wu, J. S. Speck, and S. P. DenBaars, Appl. Phys. Lett. **81**, 469 (2002); **81**, 1201 (2002).
[7]F. Wu, M. D. Craven, S. H. Lim, and J. S. Speck, J. Appl. Phys. **94**, 942 (2003).
[8]A. Chitnis, C. Chen, V. Adivarahan, M. Shatalov, E. Kuokstis, V. Mandavilli, J. Yang, and M. A. Khan, Appl. Phys. Lett. **84**, 3663 (2004).
[9]R. Sharma, P. M. Pattison, H. Masui, R. M. Farrell, T. J. Baker, B. A. Haskell, F. Wu, S. P. DenBaars, J. S. Speck, and S. Nakamura, Appl. Phys. Lett. **87**, 231110 (2005).
[10]A. Chakraborty, T. J. Baker, B. A. Haskell, F. Wu, J. S. Speck, S. P. DenBaars, S. Nakamura, and U. K. Mishra, Jpn. J. Appl. Phys., Part 2 **44**, L945 (2005).
[11]A. Chakraborty, K. C. Kim, F. Wu, B. A. Haskell, S. Keller, J. S. Speck, S. Nakamura, S. P. DenBaars, and U. K. Mishra, Jpn. J. Appl. Phys., Part 1 **45**, 8659 (2006).
[12]A. D. Hanser, L. Liu, E. A. Preble, D. Tsvetkov, M. Tutor, N. M. Williams, K. Evans, Y. Zhou, D. Wang, C. Ahyi, C. C. Tin, J. Williams, M. Park, D. F. Storm, D. S. Katzer, S. C. Binari, J. A. Roussos, and J. A. Mittereder, CS MANTECH Conference, Vancouver, British Columbia, Canada, 2006 (unpublished).
[13]A. Chakraborty, B. A. Haskell, S. Keller, J. S. Speck, S. P. DenBaars, S. Nakamura, and U. K. Mishra, Jpn. J. Appl. Phys., Part 2 **44**, L173 (2005).
[14]M. C. Schmidt, K. C. Kim, H. Sato, N. Fellows, H. Masui, S. Nakamura, S. P. DenBaars, and J. S. Speck, Jpn. J. Appl. Phys., Part 2 **46**, L126 (2007).
[15]K. Okamoto, H. Ohta, S. F. Chichibu, J. Ichihara, and H. Takasu, Jpn. J. Appl. Phys., Part 2 **46**, L187 (2007).
[16]M. C. Schmidt, K. C. Kim, R. M. Farrell, D. F. Feezell, D. A. Cohen, M. Saito, K. Fujito, J. S. Speck, S. P. DenBaars, and S. Nakamura, Jpn. J. Appl. Phys., Part 2 **46**, L190 (2007).
[17]K. Okamoto, T. Tanaka, M. Kubota, and H. Ohta, Jpn. J. Appl. Phys., Part 2 **46**, L820 (2007).
[18]Y. Naoi, K. Ikeda, T. Hama, K. Ono, R. Choi, T. Fukumoto, K. Nishino, S. Sakai, S. M. Lee, and M. Koike, Phys. Status Solidi C **4**, 2810 (2007).
[19]J. P. Liu, J. B. Limb, J.-H. Ryou, D. Yoo, C. A. Horne, R. D. Dupuis, Z. H. Wu, A. S. Fischer, F. A. Ponce, A. D. Hanser, L. Liu, E. A. Preble and K. R. Evans, Appl. Phys. Lett. **92**, 011123 (2008).
[20]T. Detchprohm, M. Zhu, Y. Xia, Y. Li, W. Zhao, J. Senawiratne, and C. Wetzel, Phys. Status Solidi C **5**, 2207 (2008).
[21]M. Tsuda, H. Furukawa, A. Honshio, M. Iwaya, S. Kamiyama, H. Amano, and I. Akasaki, Jpn. J. Appl. Phys., Part 1 **45**, 2509 (2006).
[22]T. L. Tansley and E. M. Goldys, in *Properties, Processing and Applications of Gallium Nitride and Related Semiconductors*, edited by J. Edgar, S. Strite, I. Akasaki, H. Amano, and C. Wetzel (INSPEC, IEE, London, 1999), pp. 123–128.

Downloaded 03 Sep 2009 to 128.113.121.60. Redistribution subject to AIP license or copyright; see http://apl.aip.org/apl/copyright.jsp